Hierarchical NiFeV Hydroxide Nanotubes: Synthesis, Topotactic Transformation and Electrocatalysis towards Oxygen Evolution Reaction

Qingying Li,[a] Xiaohe Liu,[a,b] Zhicheng Zheng,[a] Gen Chen,[a] Renzhi Ma,[c] Hao Wan*[b]*

[a] State Key Laboratory of Powder Metallurgy and School of Materials Science and Engineering, Central South University, Changsha, Hunan 410083, P.R. China.

[b] School of Chemical Engineering, Zhengzhou University, Zhengzhou 450001, P.R. China.

[c] World Premier International Center for Materials Nanoarchitectonics (WPI-MANA), National Institute for Materials Science (NIMS), Namiki 1-1, Tsukuba, Ibaraki 305-0044, Japan.

Corresponding Author

*E-mail: liuxh@csu.edu.cn (Xiaohe Liu).

*E-mail: wanhao@zzu.edu.cn (Hao Wan).

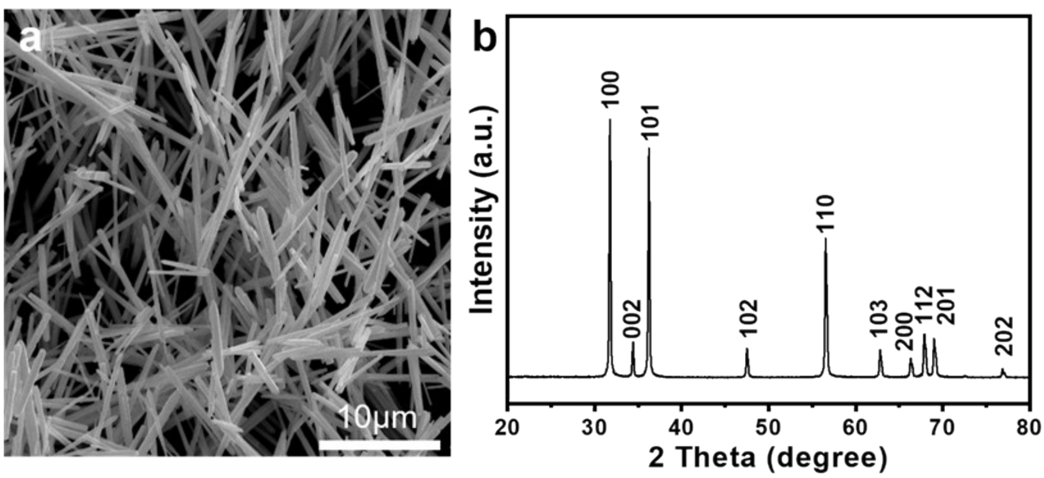

Fig. S1. (a) SEM image and (b) XRD pattern of ZnO nanorods.

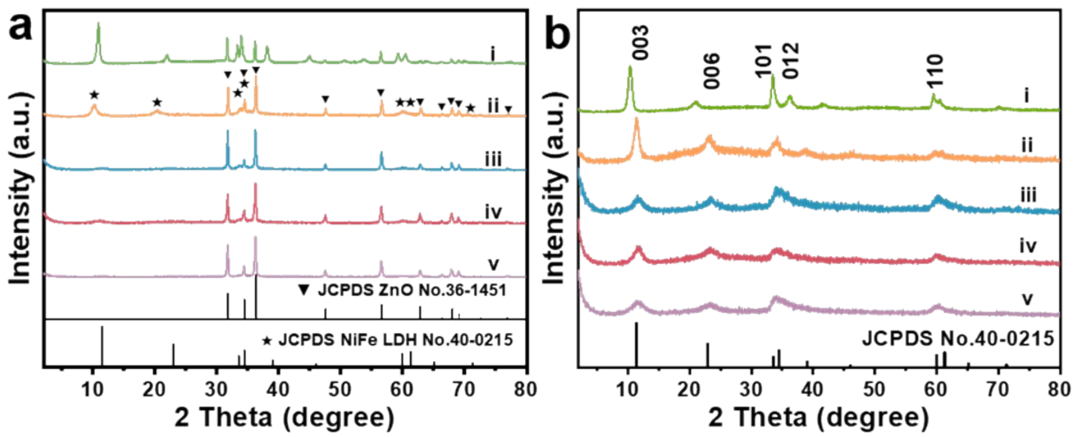

Fig. S2. (a) XRD pattern of i) $Ni(OH)_2$-CST, ii) NiFe-82 LDHs-CST, iii) NiFeV-611 LDHs-CST, iv) NiFeV-811 LDHs-CST, v) NiFeV-1011 LDHs-CST; (b) XRD pattern of i) $Ni(OH)_2$-HNT, ii) NiFe-82 LDHs-HNT, iii) NiFeV-611 LDHs-HNT, iv) NiFeV-811 LDHs-HNT, v) NiFeV-1011 LDHs-HNT.

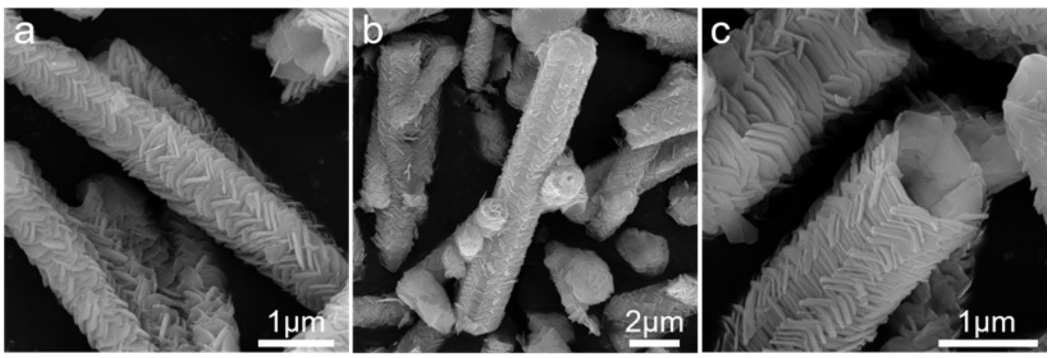

Fig. S3. (a) SEM image of $Ni(OH)_2$-CST; (b) and (c) SEM image of $Ni(OH)_2$-HNT with different magnification.

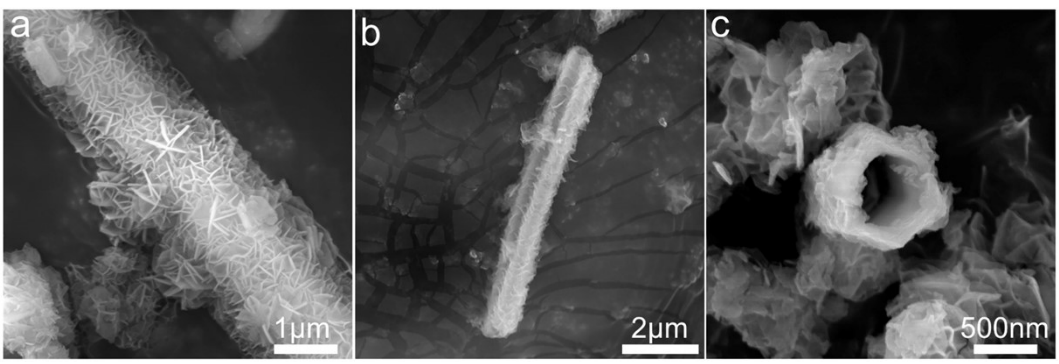

Fig. S4. (a) SEM image of NiFe-82 LDHs-CST; (b) and (c) SEM image of NiFe-82 LDHs-HNT with different magnification.

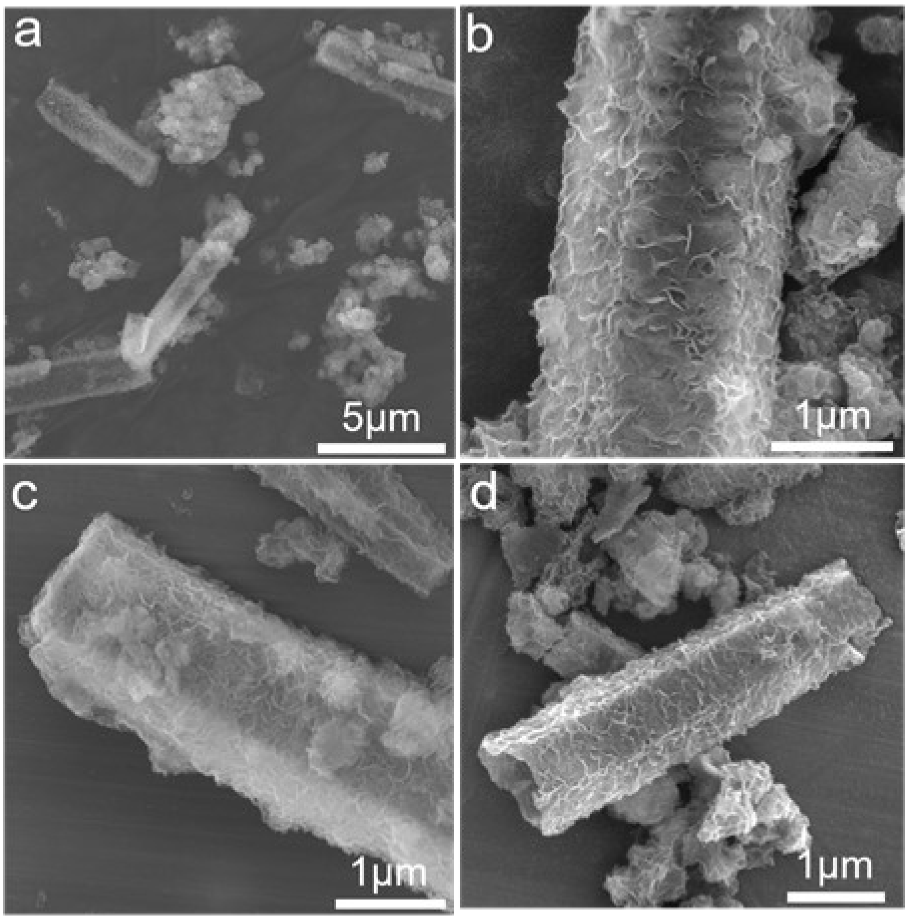

Fig. S5. SEM image of (a) NiFeV-811 LDHs-HNT with low magnification; (b) NiFeV-811 LDHs-HNT with high magnification (c) NiFeV-611 LDHs-HNT and (d) SEM image of NiFeV-1011 LDHs-HNT.

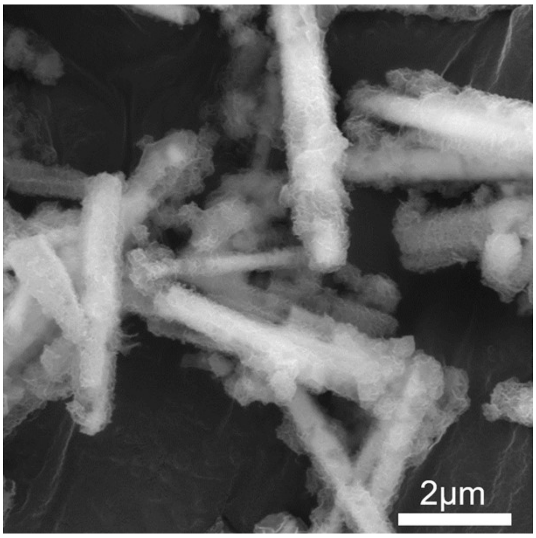

Fig. S6. SEM image of NiFeV-811 LDHs-CST.

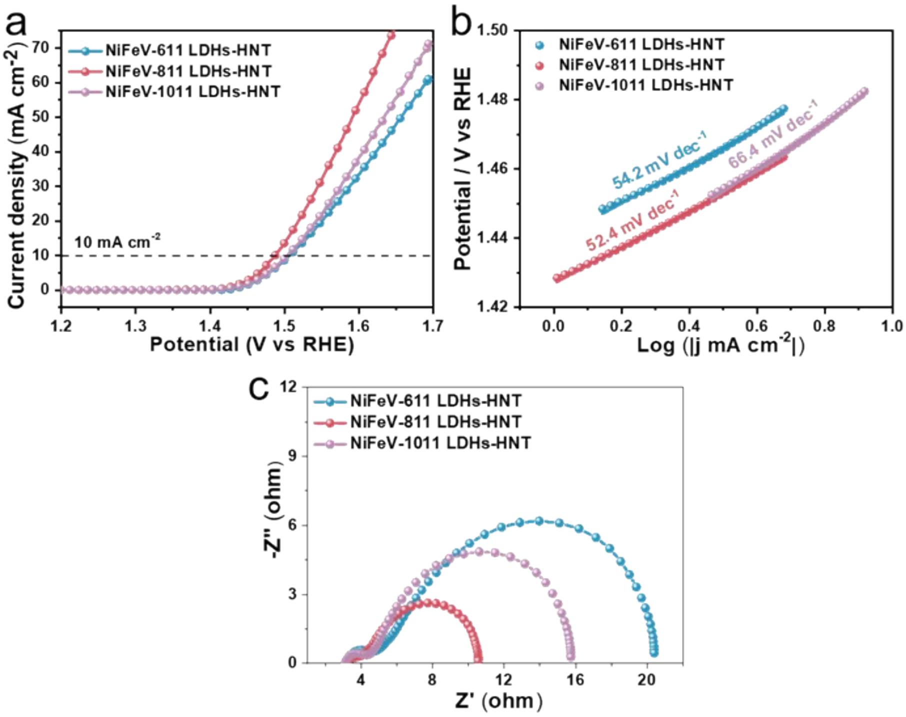

Fig. S7. Electrochemical measurement results of NiFe-611 LDHs-HNT, NiFeV-811 LDHs-HNT and NiFeV-1011 LDHs-HNT (a) LSV plots, (b) Tafel plots, (c) Nyquist plots measured at 0.55 V vs Hg/HgO.

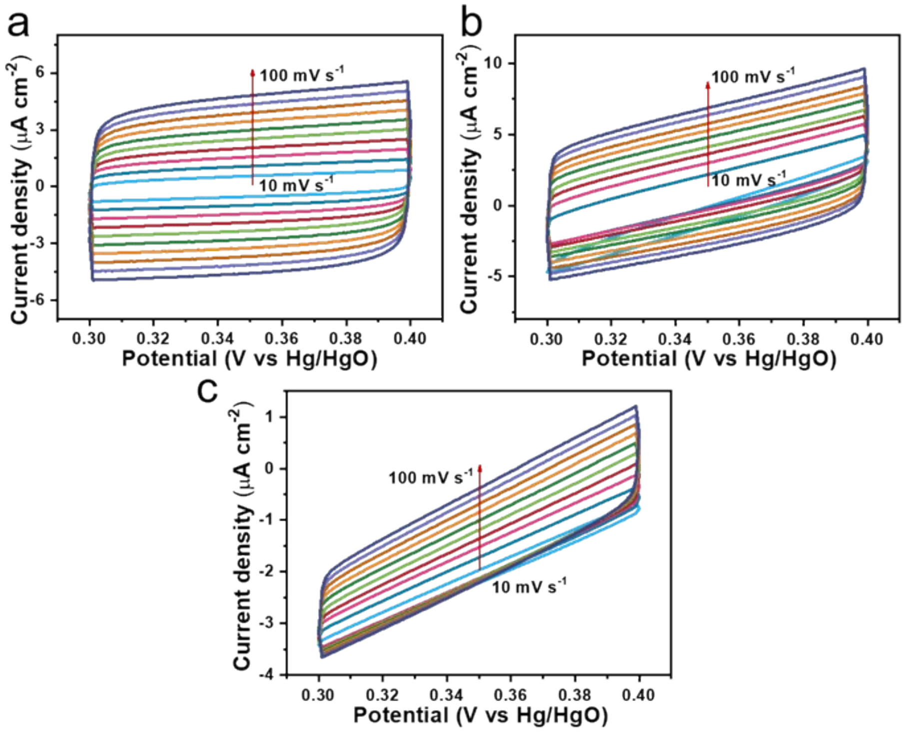

Fig. S8. The Cycle voltammograms (CV) curves of (a) NiFe-82 LDHs-HNT, (b) NiFeV-811 LDHs-HNT, (c) NiFeV-811 LDHs-CST.

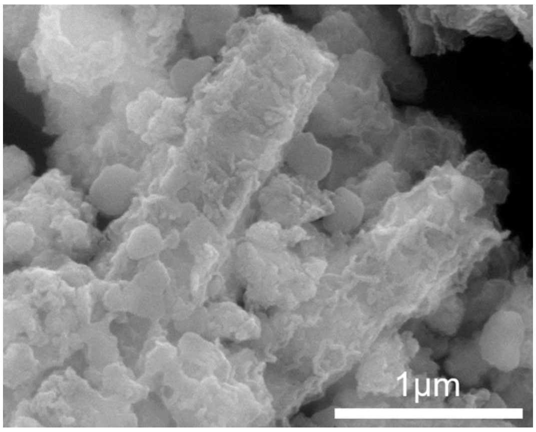

Fig. S9. SEM image of NiFeV-811 LDHs-HNT after 45h CP.

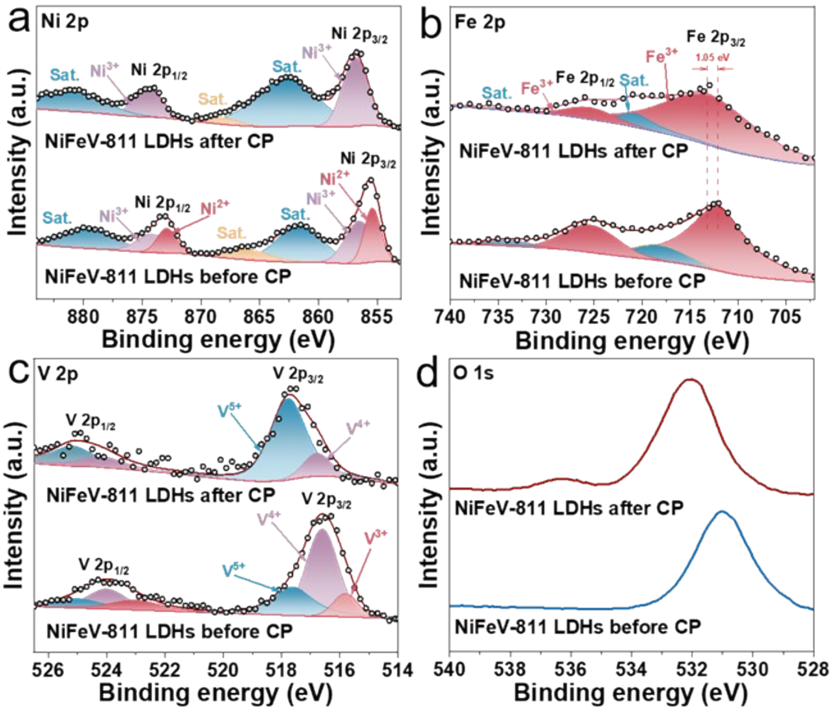

Fig. S10. High-resolution XPS spectra of NiFeV-811 LDHs HNT before and after CP measurement: (a) Ni 2p; (b) Fe 2p; (c) V 2p; (d) O 1s spectra. It can be observed that after a long time of OER process, due to the oxidation during the testing, Ni^{2+} was completely oxidized to Ni^{3+}, while the peaks of Fe 2p also shift to higher binding energy. The content of V^{5+} in V 2p shows a higher peak area after OER than the initial NiFeV-811 LDHs-HNT. In the O 1s spectra, the main peak for O 1s is shifted from 530.9 eV to 532.1 eV, which indicate that the hydroxyl group in the hydroxide is converted into peroxide group (-OOH). Meanwhile, compared to the NiFeV-811 LDHs-HNT before CP a new peak is generated at 536.2eV, which is ascribed to the oxidation of carbon fiber paper.

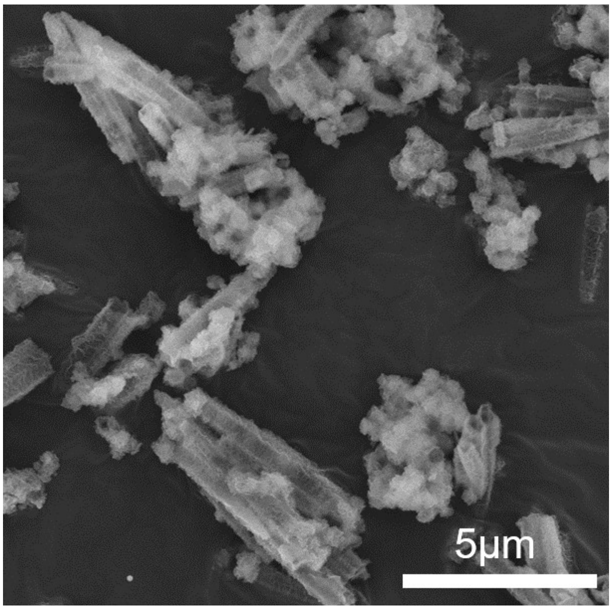

Fig. S11. SEM image of NiFeVP hollow nanotubes with low magnification.

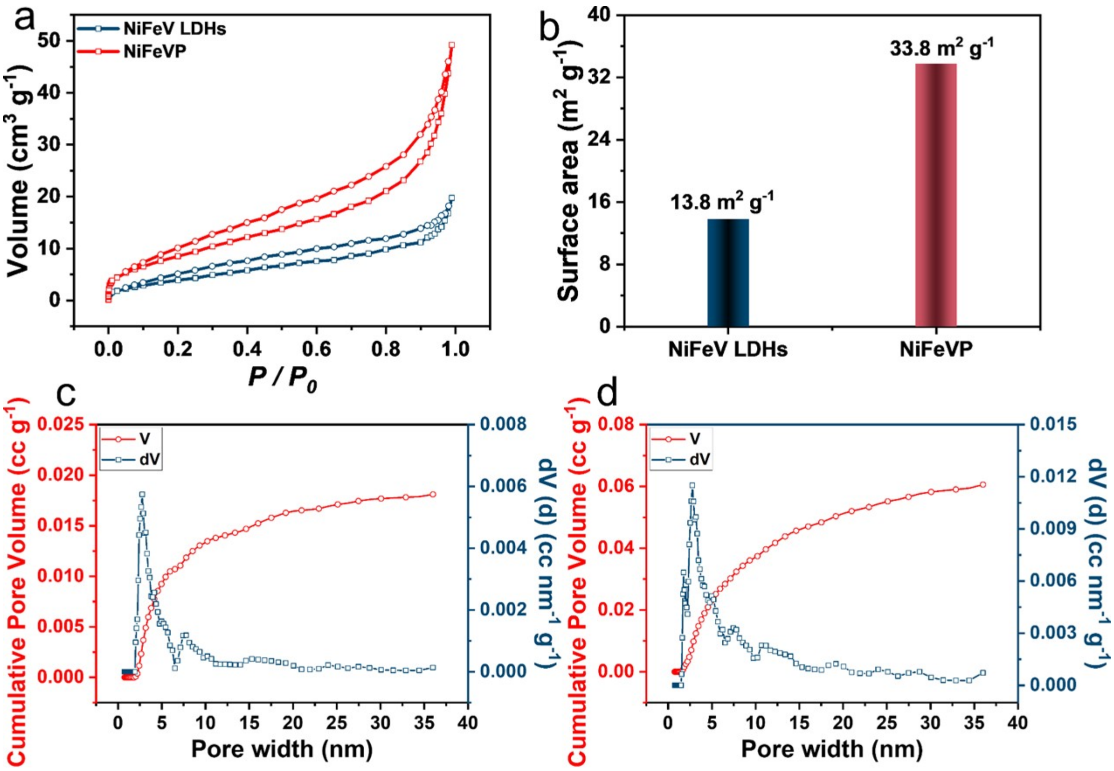

Fig. S12. Porosity analysis of NiFeV-811 LDHs HNT and NiFeVP samples. (a) N_2 sorption isotherm and (b) specific surface area. Pore structures of (c) NiFeV-811 LDHs HNT and (d) NiFeVP samples. Pore volume was estimated as 0.024 and 0.061 cc g^{-1} for NiFeV-811 LDHs-HNT and NiFeVP hollow nanotubes using DFT analysis, respectively.

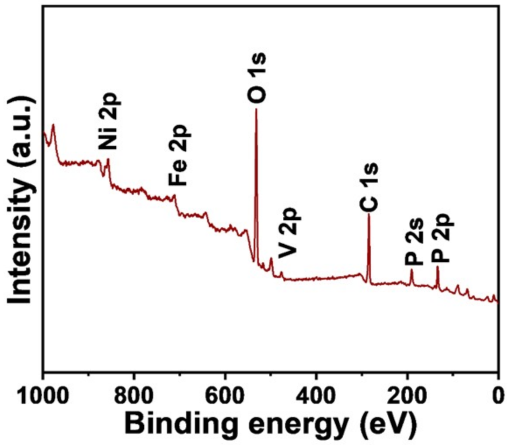

Fig. S13. Full XPS spectrum of NiFeVP hollow nanotubes.

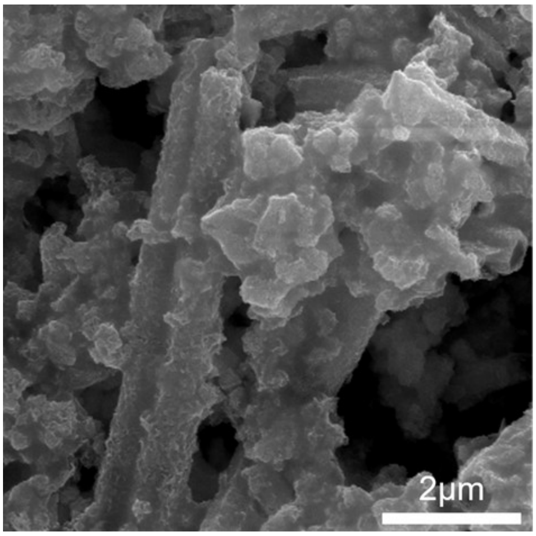

Fig. S14. SEM image of NiFeVP hollow nanotubes after 50h CP.

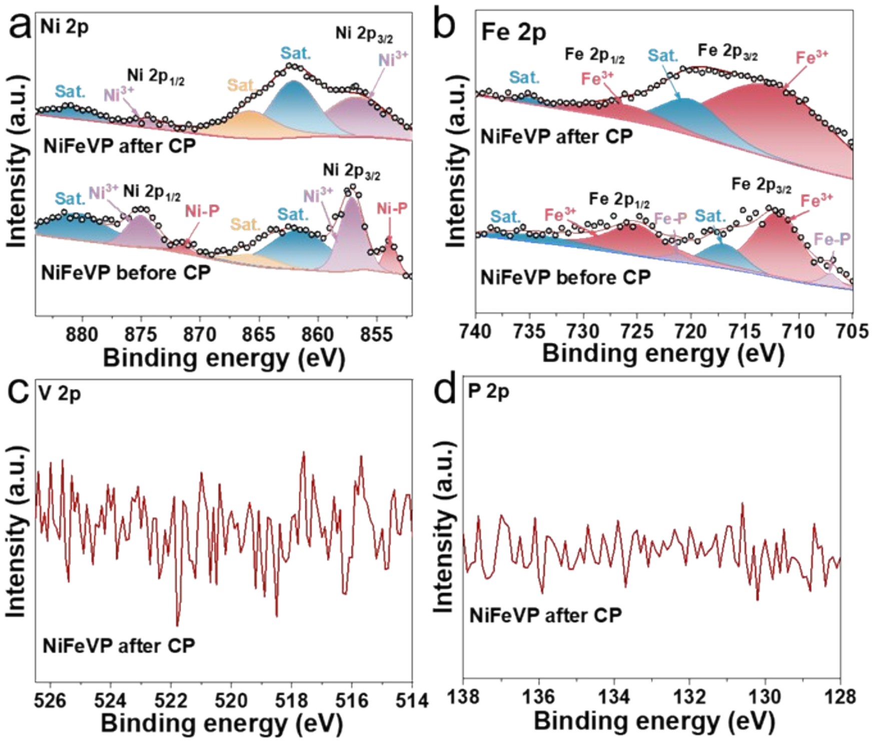

Fig. S15. High-resolution XPS spectra of NiFeVP hollow nanotubes before and after CP measurement. (a) Ni 2p, (b) Fe 2p, (c) V 2p and (d) P 2p.

Table S1. Calculated values based on the fitted equivalent circuit.

Product	Rs (Ω)	Rct (Ω)	Rp (Ω)
NiFe-82 LDHs-HNT	3.182	50.42	7.284
NiFeV-811 LDHs-HNT	3.252	6.31	1.215
NiFeV-811 LDHs-CST	2.942	51.94	16.04
NiFeVP	2.696	3.649	0.915

Table S2. Electrochemical analysis of NiFeV-811 LDHs-HNT, NiFe-82 LDHs-HNT, NiFeV-811 LDHs-CST and their intrinsic activities toward OER.

Product	Double-layer Capacitance (C_{dl}) (mF cm^{-2})	Rough Factor (R_f)	J @ 1.5 V_{RHE} (mA cm^{-2})	$J_{specific}$ @ 1.5 V_{RHE} (mA cm^{-2})
NiFeV-811 LDHs HNT	96.28	1.60	13.84	8.62
NiFe-82 LDHs HNT	91.96	1.53	6.32	4.13
NiFeV-811 LDHs CST	17.66	0.30	2.21	7.52

Table S3. Comparison of electrocatalytic performances of some representative Ni-based catalysts for OER in 1.0 M KOH.

Catalysts	Current density (mA cm^{-2})	Tafel slop (mV dec^{-1})	Overpotential (mV)	Reference
NiFeVP hollow nanotubes	10	30.3	209.5	This work
NiFeVP	10	34.4	249.0	[1]
$Ni_{1.5}Fe_{0.5}P$	10	125.0	264.0	[2]
D-Ni_5P_4|Fe	10	45.7	217.3	[3]
NiFeP	10	60.0	270.0	[4]
NiFePi/P	10	57.0	230.0	[5]
NiFe LDH @NiCoP/NF	10	48.6	220.0	[6]
V-Ni_2P/NF-AC	10	66.0	221.0	[7]
P-NiFe-800 NPs	10	39.0	270.1	[8]

References

1. Y. Jeung, H. Jung, D. Kim, H. Roh, C. Lim, J. W. Han and K. Yong, *J. Mater. Chem. A*, 2021, **9**, 12203-12213.
2. H. Huang, C. Yu, C. Zhao, X. Han, J. Yang, Z. Liu, S. Li, M. Zhang and J. Qiu, *Nano Energy*, 2017, **34**, 472-480.
3. J. Qi, T. Xu, J. Cao, S. Guo, Z. Zhong and J. Feng, *Nanoscale*, 2020, **12**, 6204-6210.
4. Z. Liu, G. Zhang, K. Zhang, H. Liu and J. Qu, *ACS Sustainable Chem. Eng.*, 2018, **6**, 7206-7211.
5. Q. Zhang, T. Li, J. Liang, N. Wang, X. Kong, J. Wang, H. Qian, Y. Zhou, F. Liu, C. Wei, Y. Zhao and X. Zhang, *J. Mater. Chem. A*, 2018, **6**, 7509-7516.
6. H. Zhang, X. Li, A. Hähnel, V. Naumann, C. Lin, S. Azimi, S. L. Schweizer, A. W. Maijenburg and R. B. Wehrspohn, *Adv. Funct. Mater.*, 2018, **28**, 1706847.
7. T. Zhao, X. Shen, Y. Wang, R. K. Hocking, Y. Li, C. Rong, K. Dastafkan, Z. Su and C. Zhao, *Adv. Funct. Mater.*, 2021, **31**, 2100614.
8. W. K. Gao, J. Q. Chi, Z. B. Wang, J. H. Lin, D. P. Liu, J. B. Zeng, J. F. Yu, L. Wang, Y. M. Chai and B. Dong, *J. Colloid Interface Sci.*, 2019, **537**, 11-19.